Screening of Aluminum-Based MOFs for Effective In Situ Immobilization of Biomolecules

Ioanna Christodoulou, Effrosyni Gkaniatsou, Nathalie Steunou, Aymric Kisserli, Jacques H. M. Cohen, Mohamed Haouas, Clémence Sicard

Screening of Aluminum-based MOFs for Effective In-situ Immobilization of Biomolecules

Ioanna Christodoulou,*[a] Effrosyni Gkaniatsou,[a] Nathalie Steunou,[a] Aymric Kisserli,[b,c] Jacques H. M. Cohen,[b] Mohamed Haouas[a] and Clémence Sicard*[a,d]

[a] *Institut Lavoisier de Versailles, UMR CNRS 8180, UVSQ, Université Paris-Saclay, 78035 Versailles, France*

[b] *Nanosciences Research Laboratory LRN EA 4682, University of Rheims Champagne-Ardenne, Rheims, France*

[c] *Oncogeriatric Coordination Unit, Rheims University Hospital, Rheims, France*

[d] *Institut Universitaire de France, Paris, France*

Correspondence: ioanna.christodoulou@sorbonne-universite.fr and clemence.sicard@uvsq.fr

ABSTRACT

An effective approach for the immobilization and protection of biological entities is their encapsulation via the in-situ synthesis of metal-organic frameworks (MOFs). To ensure the preservation of the bio-entities, mild synthetic conditions, including aqueous media and ambient conditions (temperature, pressure) are preferred. In this study, we investigated the synthesis of various aluminum polycarboxylate-based MOFs, including the fumarate, terephthalate, amino-terephthalate, and muconate forms of MIL-53(Al), as well as MIL-110 and MIL-160 MOF type. The potential as immobilization matrices was then assessed using bovine serum albumin (BSA). Finally, MIL-53(Al)-fum was selected for the encapsulation of a mixture of polysaccharides and more structurally complex bio-entities (viruses).

INTRODUCTION

Over the past decade, metal-organic frameworks (MOFs) have emerged as promising immobilization matrices for biological entities.[1,2] MOFs consist of the assembly of metal ions or oxoclusters with polydentate organic ligands via coordination bonds, forming highly porous crystalline structures.[3,4] MOFs present some remarkable properties, including tuneable chemical compositions and porosities, and adjustable hydrophilic/hydrophobic microenvironment, favoring biomolecules stabilization and protection while promoting reactants diffusion.[5–9] Among the immobilization strategies, the in-situ synthesis of the MOF in presence of the bio-entities, involving the growth of MOF particles around the targeted biomolecules, appears as a powerful strategy to encapsulate bio-entities independently of their size.[10,11] Indeed, biomolecules ranging from proteins to viruses and cells have been successfully encapsulated.[12–14] Nevertheless, this methodology restricts the range of synthetic conditions to a narrow window compatible with the requisite conditions for bio-entities (i.e., water, mild temperatures). Such conditions strongly limit the number of MOFs and were initially mostly reported for Zn-imidazolate-based frameworks.[10–17] However, major efforts are currently being made to broaden the selection of MOF and other structures have been successfully used. For instance, the mesoporous MIL-100(Fe) (MIL = Matériaux Institut Lavoisier) was synthesized in presence of proteins or as a bacteria exoskeleton.[18,19] Other types reported, for the in-situ immobilization of large enzymes under mild conditions, include MIL-53(Al)-NH_2, MOF-74(Zn), Fe-fumarate and HKUST(Cu).[20–23] All these studies demonstrated the relevance and interest of expanding the library of in-situ encapsulation.

Inspired by a study that screened various metals (Al-, Zn-, Cu-, Ni-, Zr-) associated with benzene-1,4-dicarboxylate and biphenyl-4,4'-dicarboxylate linkers,[24] we hypothesized that investigating the effect of different ligands of MOFs while keeping the same metal might be relevant, especially for isoreticular MOFs. In this vein, aluminum was chosen as metal source, as it is abundant and inexpensive and a well-known immune-stimulant metal used in adjuvanted vaccines, and as it will enable to probe the MIL-53(Al) series.[25-28] MIL-53(Al) structures consist of 1D $AlO_4(OH)_2$ chains of corner sharing Al(III) octahedra linked by linear dicarboxylates (terephthalate, fumarate, muconate, etc..).[29–31] The ligand can also be substituted with functional groups (e.g. $–NH_2$).[32] A remarkable feature of most of the MIL-53 series is their structural flexibility and their controlled modulation by external stimuli (e.g. host

in the pores, temperature, pressure, humidity, synthetic conditions, etc.). The framework can be subjected to different pore closing/opening constraints, ranging from a fully closed pore configuration to a fully open/large pore configurations, via intermediate situations, also described as the breathing effect, of high interest for many applications such as gas separation.[33]

Herein, to expand the chemical composition and structural features of MOFs used for the in-situ bio-encapsulation, we have examined the green synthesis in aqueous medium at room temperature under atmospheric pressure of several types of MIL-53, namely MIL-53(Al)-fum,[30] MIL-53(Al),[29] MIL-53(Al)-NH_2,[32] and MIL-53(Al)-muc[31] using fumarate (or trans-butenedioate), terephthalate (or 1,4-benzenedicarboxylate), amino-terephtalate (or 2-amino-1,4-benzenedicarboxylate), and muconate (or trans,trans-1,3-butadiene-1,4-dicarboxylate) as linker, respectively. We have extended the investigation to the tricarboxylate trimesate linker (1,3,5-benzene tricarboxylate) with which several Al-frameworks can be obtained, including MIL-96(Al),[34,35] MIL-100(Al)[36] and MIL-110(Al),[37] as well as to 2,5-furandicarboxylate leading to MIL-160(Al).[38] We then explored their potential for the encapsulation of bovine serum albumin (BSA), a widely studied protein (Scheme 1). Among the different MOFs, MIL-53(Al)-fum was chosen as the most promising, based on its crystallinity, purity and immobilization efficiency (> 98%), and was further used as a platform for immobilizing a mixture of polysaccharides and viruses.

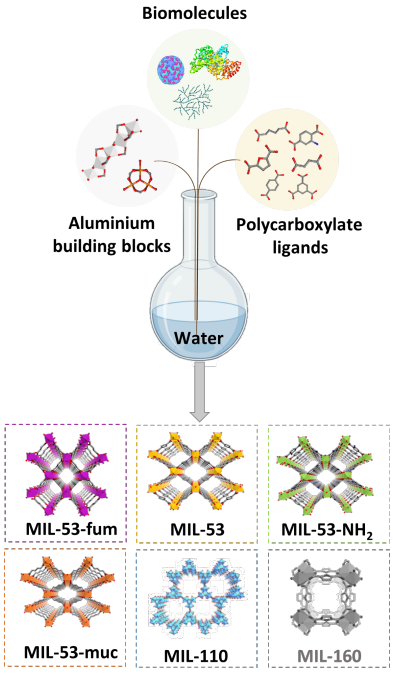

Scheme 1. Schematic representation of the screening of various Al-based polycarboxylates MOF structures.

RESULTS AND DISCUSSION

Screening of Al-polycarboxylate MOFs

Among the dicarboxylate linkers leading to MIL-53(Al) structures (Table S1, in the ESI), we selected fumaric acid (trans-butenedioic acid), terephtalic acid (1,4-benzenedicarboxylic acid), amino-terephtalic acid (2-amino-1,4-benzenedicarboxylic acid), muconic acid (trans, trans-1,3-butadiene-1,4-dicarboxylic acid) based on their relative higher water solubility compared to other ligands. The crystallographic parameters of each corresponding structure, i.e. **MIL-53(Al)-fum, MIL-53(Al), MIL-53(Al)-NH_2,** and **MIL-53(Al)-muc**, respectively, are summarized in Table S1. As shown in Figure 1a-e, all of the linkers led to the formation of a crystalline phase in water at room temperature. **MIL-53(Al)-fum** exhibited powder X-ray diffraction (PXRD) pattern close to the calculated one,[30] suggesting its successful formation in aqueous media under ambient conditions (Figure 1a). The PXRD pattern of **MIL-53(Al)** aligned well with the calculated one of MIL-53(Al) with unreacted ligand within the pores,[29] indicating the washing steps were not sufficient to remove the unreacted ligand (Figure 1b). This can be explained by the low aqueous solubility of the linker as washing steps were performed in H_2O to preserve the bio-entities' integrity once incorporated. **MIL-53(Al)-NH_2** displayed PXRD pattern in agreement with the calculated one of the hydrated form of the MOF (Figure 1c).[32] Both **MIL-53(Al)** and **MIL-53(Al)-NH_2** displayed broad Bragg peaks suggesting a moderate crystallinity or structural heterogeneity maybe resulting from a mixture of different microdomains with various pore openings. **MIL-53(Al)-muc** also exhibited a PXRD pattern in agreement with the calculated one (Figure 1d).[31] When using the tricarboxylate trimesate linker a mixture of two phases, **MIL-96(Al)** and **MIL-110(Al)** were obtained (Figure 1e). The synthesis using 2,5-furandicarboxylate yielded **MIL-160(Al)** (Figure S1), however, some extra Bragg Peak can be observed on the PXRD pattern, suggesting the presence of an impurity. Moreover, the reaction time needed for the formation of this MOF was 72 hours. This duration is not recommended for the preservation of bio-entity activity, so MIL-160(Al) was not selected for further studies with bio-entities.

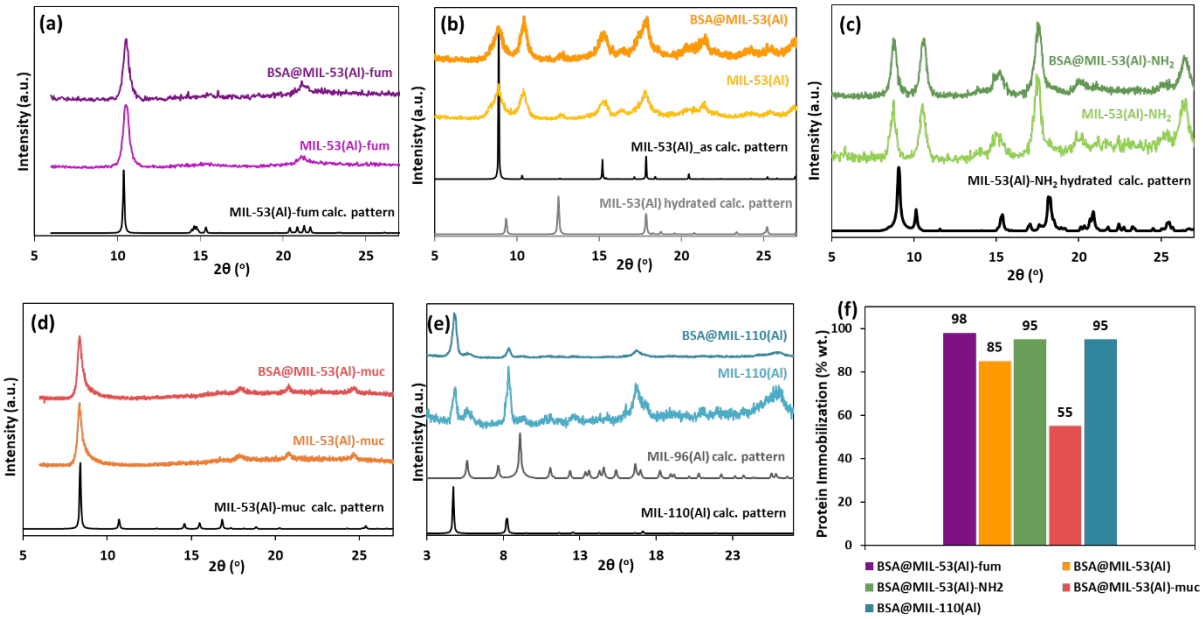

Figure 1. PXRD patterns of a) MIL-53(Al)-fum, b) MIL-53(Al) (as = as synthesized with unreacted ligand in the pores), c) MIL-53(Al)-NH_2, d) MIL-53(Al)-muc and e) MIL-110(Al) in the absence or presence of BSA. f) BSA immobilization efficiency quantified by the amount of BSA detected in the supernatant (not adsorbed BSA), using the µBCA protein determination assay.

Immobilization of BSA

To verify the efficiency of these MOFs as platforms for encapsulation of bio-entities, the protein, bovine serum albumin (BSA) was chosen as a model. BSA (molecular weight of 66.5 kDa) is made up of a single chain of amino acids and is one of the most abundant proteins in blood.[39] The PXRD patterns of MOFs obtained in presence of BSA confirmed the preservation of their crystalline structures (Figure 1 a-e). For all the MIL-53 types, **BSA@MIL-53(Al)-fum, BSA@MIL-53(Al), BSA@MIL-53(Al)-NH_2, BSA@MIL-53(Al)-muc**, the presence of BSA during the synthesis did not influence the crystallinity of the obtained material. Interestingly, the presence of BSA in the Al-trimesates synthesis mixture not only improves the crystallinity of **BSA@MIL-110(Al)**, but also prevents the formation of MIL-96. This observation suggests a biomimetic mineralization process may be occurring, similar to what has previously been reported with ZIF-8.[11] The surface of the BSA protein could concentrate the Al^{3+} cation favoring the formation of MIL-110's building unit over MIL-96's one.[40]

To determine whether BSA had been immobilized during synthesis, the amount of BSA remaining in the synthesis supernatant was assessed, via µBCA assay (Figure S2). As

shown in Figure 1f the detected protein in the supernatants for **BSA@MIL-53(Al)-fum** and **BSA@MIL-53(Al)-NH_2** was negligible (immobilization efficiency ~ 98 and 95 % respectively). In the case of **BSA@MIL-53(Al)** the efficiency was lower, but still very satisfactory (~ 85 %), while **BSA@MIL-53(Al)-muc** presented the lowest value of all MOFs (~ 55 %). Thus, the **MIL-53(Al)-muc** was not selected for the immobilization of other biomolecules.

Based on the crystallinity, phase purity and excellence BSA immobilization performance **MIL-53(Al)-fum** was the MOF of choice for further investigations, and similar experiments were performed by increasing the amount of BSA introduced in the synthesis reaction. BSA solution (3 mg/mL) was added to the reaction as aliquots, corresponding to protein amounts of 0.15 mg, 0.225 mg and 0.45 mg. After protein's immobilization, the dried powder was characterized by PXRD and the supernatants by μBCA protein determination assay (Figure 2).

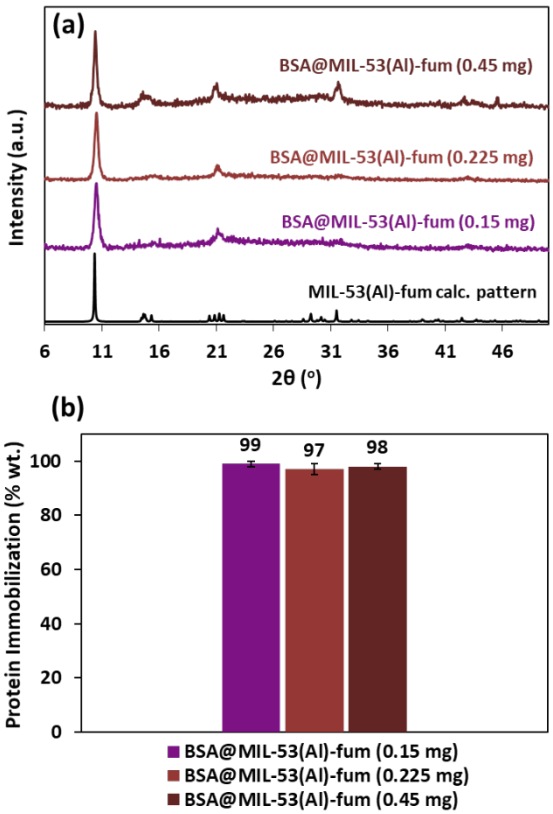

Figure 2. PXRD patterns of a) MIL-53(Al)-fum synthesized in presence of BSA protein at different concentrations, b) Determination of immobilization efficiency of the BSA at different concentrations, using the μBCA protein determination assay.

The structural integrity of the encapsulated protein was evaluated by SDS-PAGE electrophoresis. To do so, BSA was released from **BSA@MIL-53(Al)-fum** after incubating the solid in a solution containing EDTA and PBS (phosphate buffer saline) overnight, leading to the degradation of the solid. The resulting solution was analyzed as well as the synthesis supernatant. As seen in Figure 3, the released BSA (lane 2) migrated similarly as the BSA band of the non-encapsulated Biorad kaleidoscope® molecular weight ladder (lane 1), indicating a similar molecular weight and (lane 1), indicating a similar molecular weight and the absence of degradation of the structure. The synthesis supernatant did not contain any BSA (lane 3), in agreement with the µBCA assay.

The obtained PXRD patterns consistently indicated the formation of **BSA@MIL-53(Al)-fum**, regardless of the varying BSA concentrations (Figure 2a). Very importantly, almost no protein was detected in the supernatant (immobilization efficiency ~ 98), even when the highest amount of BSA was introduced during the synthetic procedure (0.45 mg) (Figure 2b).

Overall, these results highlight the high potential of **MIL-53(Al)-fum** for the immobilization of proteins.

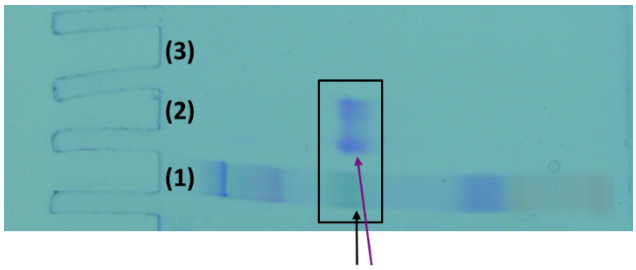

Figure 3. SDS-PAGE gel, BSA is highlighted by a square, lane 1: molecular weight ladder (BSA is stained in green, black arrow), lane 2: BSA released from BSA@MIL-(53)Al-fum powder (purple arrow), lane 3: synthesis supernatant of BSA@MIL-(53)Al-fum, lane devoid of BSA.

Immobilization of polysaccharides in MIL-53(Al)-fumarate

The relevance of the synthesis for immobilizing a mixture of polysaccharide molecules was also assessed. To demonstrate a proof of concept for potential vaccine application, pneumococcal polysaccharides presented in the commercialized vaccine PNEUMOVAX® were selected. PNEUMOVAX® is a 23-valent vaccine designed to prevent Pneumococcal disease and each vaccine dose (0.5 mL) contains 25 µg of each 23

pneumococcal polysaccharide serotypes (1, 2, 3, 4, 5, 6B, 7F, 8, 9N, 9V, 10A, 11A, 12F, 14, 15B, 17F, 18C, 19F, 19A, 20, 22F, 23F, 33F) and its recommended storage temperature is between 2-8°C due to the thermal instability of the formulation.[41]

The addition of the polysaccharide mixture within the synthesis did not impede the formation of MIL-53(Al)-fum as demonstrated by the PXRD pattern displayed in Figure 4, but some low intensity extra Bragg peaks could be observed at 22.7°, 23.9°, 23.8°, 25.6°, which may suggest traces of impurities.

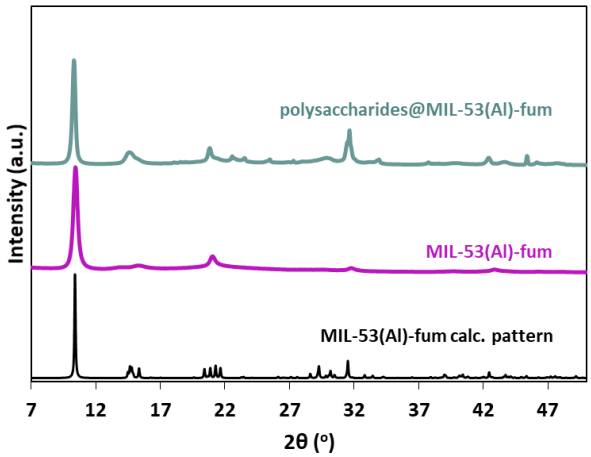

Figure 4. PXRD patterns of MIL-53(Al)-fum synthesized in aqueous medium at room temperature in the presence and absence of polysaccharides.

To further investigate the obtained structure, solid-state NMR spectroscopy was performed (Figure 5a,b and S3-S5). ^{1}H, ^{13}C and ^{27}Al NMR spectra displayed significant differences between **MIL-53(Al)-fum** and **polysaccharides@MIL-53(Al)-fum**. ^{1}H NMR spectra revealed a higher content of adsorbed water molecules in **polysaccharides@MIL-53(Al)-fum** in comparison to **MIL-53(Al)-fum** (Figure S3).[30] This difference in hydration rate could be due to a difference in drying conditions, but may also be attributed to the high hydrophilic nature of polysaccharides, and could explain the collapse of the structural Al-OH-Al hydroxyl group signal at 1.9 ppm, involved in the dynamic exchange with adsorbed water.

$^{13}C\{^{1}H\}$ CPMAS NMR spectrum of **MIL-53(Al)-fum** displayed two main peaks at 170.8 and 137.5 ppm attributed to the Csp^2 of the carboxyl and ethylene functions, respectively of the fumarate ligand (Figure 5a). In the spectrum of

polysaccharides@MIL-53(Al)-fum, both these two peaks are doubled, representative of two types of fumarate due to hydrated form and dehydrated form of **MIL-53(Al)-fum**, as previously reported,[30] and in agreement with ^{1}H NMR spectra. Peaks of low intensity were also observed at 166.9 and 134.2 ppm indicative of unreacted fumarate. High-power decoupling (HPDec) $^{13}C\{^{1}H\}$ MAS NMR spectrum was recorded and allowed to quantify the proportion of each compound: 50 % dehydrated form, 42 % hydrated form and 8 % unreacted fumarate (Figure S4). Due to the low sensitivity of the direct polarization technique, it was not possible to detect the embedded polysaccharides in the HPDec spectrum. However, close inspection of the $^{13}C\{^{1}H\}$ CPMAS spectrum of **polysaccharides@MIL-53(Al)-fum** reveals characteristic Csp^3 peaks due to the sugar units at 71.7 ppm, confirming the presence of polysaccharides in the **polysaccharides@MIL-53(Al)-fum** sample and their successful immobilization (Figure 5a). Using the multi-CP technique (contact time = 5 x 0.5 ms), quantification can become possible,[42] and an estimation of polysaccharide loading can be derived from this spectrum providing a glucose unit/fumarate ligand of ca. 1/150.

The ^{27}Al MAS NMR of the **polysaccharides@MIL-53(Al)-fum** sample, given in Figure 5b, shows a complex spectrum in the approximate range +5 to -100 ppm, which corresponds to the superposition of several signals. To identify and verify the signals present, an MQMAS spectrum was recorded and is shown in Figure S5. This spectrum confirms after deconvolution that three different aluminum types are present in the sample, and allows the quadrupolar parameters of their resonances to be extracted accurately. A first signal at 1.5 ± 01 ppm with a quadrupole constant Cq of 4.7 ± 02 MHz corresponds to unreacted aluminum. The other two signals at 1-3 ppm with much higher Cq in the 9-11 MHz range are characteristic of MOF-type aluminum carboxylate with corner-sharing Al-chains.[43] They correspond to the dehydrated and the hydrated forms of **MIL-53(Al)-fum**, given their respective Cq values of 9 and 11 MHz, in accordance with previous work.[30] These signals represent 10, 39 and 51 % respectively, and the ratio between hydrated and dehydrated form is close to 1:1 in line with the ^{13}C NMR results (within ± 20 %). These data suggest that the presence of the polysaccharides may favor the hydrated form of **MIL-53(Al)-fum**, possibly due to their hydrophilic nature.

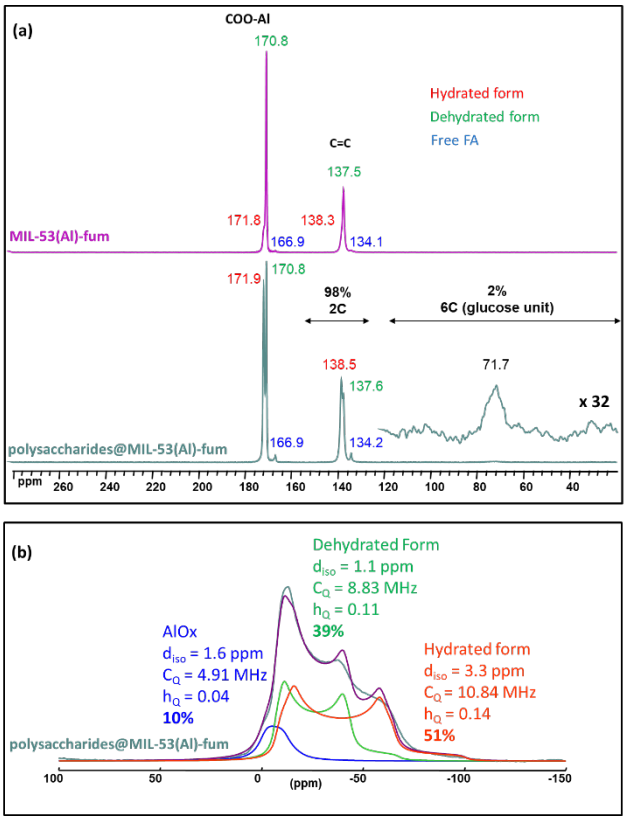

Figure 5. Solid-state NMR spectra at 20 kHz MAS of polysaccharides@MIL-53(Al)-fum: a) $^{13}C\{1H\}$ CPMAS and b) ^{27}Al MAS. The spectral decomposition is based on the MQMAS spectrum shown in the ESI.

Immobilization of inactivated poliovirus in MIL-53(Al)-fum

The relevance of the process to encapsulate structurally more complex bio-entities was evaluated toward a virus. Poliomyelitis virus was selected to also serve as a proof of concept for vaccine application. Poliovirus is a typical picornavirus with a small non-lipid-containing virion approximately 27 nm in diameter. The icosahedral particle consists of sixty copies of each of the capsid proteins VP1, VP2, VP3 and VP4, encasing a single strand of messenger RNA. Polioviruses occur as serotypes 1, 2 and 3. IMOVAX® POLIO vaccine served as the source of inactivated poliomyelitis virus. One dose (0.5 mL) contains inactivated Poliomyelitis virus: type 1 (Mahoney strain produced on VERO cells) 40 D-antigen Unit (DU), type 2 (MEF-1 strain produced on VERO cells) 8 DU, and type 3 (Saukett strain produced on VERO cells) 32 DU.

PXRD patterns confirmed the formation of **polio@MIL-53(Al)-fum** (Figure 6a). When the vaccine formulation was directly added to the synthesis mixture, the immobilization capacity was around 50 % (Figure 6b). Vaccine formulations, such as in the case of IMOVAX®, contain many additives that could interfere with the synthesis. To solve this issue, the vaccine formulation was transferred to a NaCl solution using a desalting column with a molecular weight cut-off of 7 000 Da. The amount of virus immobilized within **polio@MIL-53(Al)-fum** was 63 % (Figure 6b). The increase in the total amount immobilized suggests that the presence of additives in the initial vaccine formulation can influence the immobilization process. Finally, TEM images provided additional evidence for the successful immobilization of the virus. Specifically, the microscopic images show a MOF coating around individual poliovirus (Figure 6c-d).

These data suggest that **MIL-53(Al)-fum** can be suitable not only for the immobilization of proteins but also for polysaccharides and viruses.

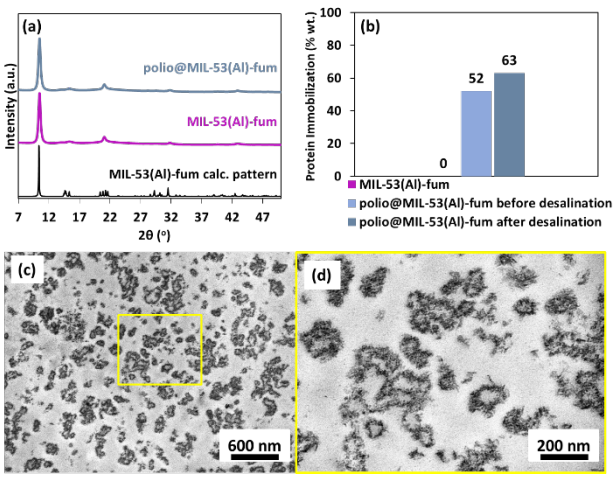

Figure 6. a) PXRD patterns of MIL-53(Al)-fum synthesized in aqueous medium at room temperature in the presence and absence of poliovirus b) Immobilization efficiency of MIL-53(Al)-fum with polio vaccinal formulation and with desalinated polio vaccinal formulation, as determined by µBCA protein determination assay, c,d) TEM images of polio@MIL-53(Al)-fum at two different magnifications.

CONCLUSION

Al-based polycarboxylate MOFs, and more precisely, a MIL-53(Al) series based on dicarboxylate ligands (**MIL-53(Al)-fum, MIL-53(Al), MIL-53(Al)-NH_2,** and **MIL-53(Al)-muc**) as well as **MIL-110(Al)** and **MIL-160(Al)** were prepared via "green" routes (aqueous media, room temperature). The efficiency of the synthetic process to immobilized bio-entities was

evaluated towards the model protein **BSA** for **MIL-53(Al)-fum, MIL-53(Al) MIL-53(Al)-NH_2, MIL-53(Al)-muc** and **MIL-110(Al)**. The selected MOFs could form in presence of BSA, and even with a higher crystallinity in the case of MIL-110. All candidates presented a high immobilization efficiency, reaching the value of 98 % with **BSA@MIL-53(Al)-fum**. The crystallinity and immobilization efficiency were maintained independently of the amount of BSA introduced in the synthesis. Thus, this MOF was selected as the most promising candidate for the immobilization of more complex bio-entities, and in particular, a mixture of pneumococcal polysaccharides and a second made up of inactivated polioviruses. We demonstrated that none of the bio-entities hampered the formation of **MIL-53(Al)-fum**. Solid-state NMR spectroscopy allowed to highlight that the presence of polysaccharides favored the formation of the hydrated form of **MIL-53(Al)-fum**, attributed to the hydrophilic nature of the polysaccharides.

These results are very promising, revealing the ability of this series of MOFs for the immobilization of complex bio-entities, opening new pathways in the biomedical field, and especially in vaccinal applications.

EXPERIMENTAL SECTION

Materials and methods

Aluminum sulfate, fumaric acid (trans-butenedioic acid), trimesic acid (1,3,5-benzenetricarboxylic acid), amino-terephtalic acid (2-amino-1,4-benzenedicarboxylic acid), 2,5-furandicarboxylic acid, sodium hydroxide, QuantiPro™ BCA Assay Kit, Phosphate buffered saline (PBS) tablet, and ethylenediaminetetraacetic acid (EDTA) were purchased from Sigma-Aldrich. Aluminum acetate, basic, 90% was obtained from Acros Organics. Terepthalic acid (1,4-benzenedicarboxylic acid) and muconic acid (trans, trans-1,3-butadiene-1,4-dicarboxylic acid) were purchased from Alfa Aesar. Bovine serum albumin, Zeba™ spin desalting column (7k MWCO, 2 mL), were purchased from Thermo Fisher Scientific. IMOVAX® POLIO vaccine from Sanofi Pasteur was used as a source of inactivated poliomyelitis virus. One dose (0.5 mL) contains inactivated Poliomyelitis virus: type 1 (Mahoney strain produced on VERO cells) 40 D-antigen Unit (DU), type 2 (MEF-1 strain produced on VERO cells) 8 DU, and type 3

(Saukett strain produced on VERO cells) 32 DU. PNEUMOVAX® vaccine from MSD was used as a source of pneumococcal capsular polyoside. One dose (0.5 mL) contains 25 µg of each 23 pneumococcal polysaccharide serotypes (1, 2, 3, 4, 5, 6B, 7F, 8, 9N, 9V, 10A, 11A, 12F, 14, 15B, 17F, 18C, 19F, 19A, 20, 22F, 23F, 33F).

Powder X-Ray diffractograms (PXRD) were measured on a Siemens D5000 Diffractometer working in Bragg-Brentano geometry [(θ-2θ) mode] by using CuKα radiation (λKα = 1.5406 Å). Solid-state NMR spectra were registered on a Bruker AVANCE NEO 500WB spectrometer using a 2.5 mm Bruker H/X double-channel MAS WVT probe and operating at 500.2 MHz frequency for ^{1}H, 125.8 MHz for ^{13}C, and 130.3 MHz for ^{27}Al. The spinning rates were 20 kHz. The ^{1}H and ^{13}C HPDec MAS (20 kHz) NMR spectra were recorded using a 90°-180°-90° Hahn-echo sequence, with inter-pulse delay synchronized with one rotor period. The 90º pulse lengths were set to 1.9 and 3.0 µs for ^{1}H and ^{13}C, respectively. The ^{1}H-^{13}C cross-polarization (CPMAS) NMR spectra were recorded using a Multi-CP sequence with 2.5 (5 x 0.5) ms contact time, and radio-frequency (rf) fields of 55 kHz on ^{13}C and 75 kHz on ^{1}H channel. ^{1}H SPINAL-64 decoupling (rf of 100 kHz) was used during acquisition of the ^{13}C HPDec and CPMAS NMR spectra. The ^{27}Al MAS (20 kHz) NMR spectra were recorded using a single 15° pulse sequence, accumulating ca 8000 scans. The 3QMAS experiment was recorded using a z-filter sequence. Chemical shifts were reported in parts per million and were referenced to TMS for ^{1}H and ^{13}C, while the ^{27}Al chemical shifts were referenced to an 0.1 M solution of $Al(NO_3)_3$ at 0 ppm. The spectra were analyzed using the DMfit software.[44]

Synthesis of MIL-53 type MOFs

The MOFs (**MIL-53(Al)-fum, MIL-53(Al), MIL-53(Al)-NH2 and MIL-53(Al)-muc)** were synthesized by mixing an aqueous solution of $Al_2(SO_4)_3$ with an aqueous solution of the corresponding carboxylate ligand with a molar ratio Metal:Ligand:H_2O of 1:2:555. The mixture was left under stirring at room temperature for 8 h, at atmospheric pressure.

Synthesis of Al-trimesate MOF (MIL-110)

The MOF was synthesized by mixing an aqueous solution of $Al_2(SO_4)_3$ with an aqueous solution of trimesate with a molar ratio Metal:Ligand:H_2O of 1:2:1111. The mixture was left under stirring at room temperature for 24 h, at atmospheric pressure.

Synthesis of MIL-160(Al)

$Al(OH)(CH_3COO)_2$, 2,5-furandicarboxylic acid and H_2O were mixed with a molar ratio of 1:1:111. The mixture was left under stirring at room temperature for 72 h.

All products were recovered by centrifugation, washed 3 times with water and dried at 100 °C overnight.

Immobilization of BSA within Al-polycarboxylate MOFs

The same synthesis procedure was followed than for the pristine MOFs, except that a solution of BSA solution (3 mg/mL) was added to the reaction a few seconds after mixing the metal and the ligand solutions together. At the end of the respective reaction time, the mixture was centrifuged and the synthesis supernatant was collected to quantify the amount of BSA remaining (not adsorbed by the MOFs), *via* µBCA protein determination assays.

SDS-PAGE of released BSA

BSA@MIL-53(Al)-fum was incubated overnight under stirring in 100 mM EDTA, 10 mM PBS pH 7.4, resulting in the degradation of the **MIL-53(Al)-fum** solid and released of the entrapped protein. The resulting solution was analyzed by electrophoresis in SDS PAGE gel.

Immobilization of polysaccharides in MIL-53(Al)-fum

Prior to use, the PNEUMOVAX® vaccine solution was lyophilized and redispersed in 50 µL MilliQ H_2O, and was then added to the reaction mixture a few seconds after mixing together the metal and ligand solutions. The final mixture was left under stirring at room temperature for 8 h. The product (**polysaccharides@MIL-53(Al)-fum**) was recovered by centrifugation. The same procedure was also performed with the addition 50 µL H_2O instead of polysaccharides solution, as a control experiment (**MIL-53(Al)-fum**). The final products were dried at 100 °C overnight and analysed.

Immobilization of inactivated polioviruses in MIL-53(Al)-fum

Prior to immobilization, IMOVAX® POLIO solution was desalted using a 2 mL Zeba Spin column (7k MWCO) to a NaCl 0.9 % solution. The presence of poliovirus was verified by the UV-Vis spectroscopy at 269 nm (Figure S6). The passed-through solution was used for the immobilization process. The same synthetic procedure was followed than for the pristine **MIL-**

53(Al)-fum, except that after mixing the metal and ligand solutions together, IMOVAX® POLIO solution was added to the reaction. The final mixture was left under stirring at room temperature for 8 h. The product (**polio@MIL-53(Al)-fum**) was recovered by centrifugation. The same procedure was also performed with the addition of H_2O instead of IMOVAX® POLIO solution, as a control experiment (**MIL-53(Al)-fum**). The final products were dried at 100 °C overnight and analyzed. The supernatants were collected to quantify the amount of virus remaining in solution, via µBCA protein determination assays, using IMOVAX® POLIO solution as a control.

Supporting Information:

Description of MOF structures and principal crystallographic parameters, MIL-160 PXRD, BCA calibration curves, solid-state NMR ^{1}H, ^{13}C, ^{27}Al (PDF)

Author Contributions

I.C.: Conceptualization, Investigation, Writing – original draft; E.G: Conceptualization, Investigation; N.S: Conceptualization, A.K: Conceptualization, Investigation; J.H.M.C. Conceptualization, Investigation, Funding acquisition, Supervision; M.H. Conceptualization, Investigation, Writing – review & editing; C.S. Conceptualization, Investigation, Funding acquisition, Supervision, Writing – review & editing. All authors edited versions of the manuscript, read, and approved the final manuscript.

Conflicts of interest

E.G., J.H.M.C., and C.S. are inventors of a patent application that describes the use of Al-MOF as a vaccine adjuvant.

Acknowledgements

The authors thanks Chakib Djediat for TEM experiments performed at the Plateau technique de Microscopie Electronique du Muséum National d'Histoire Naturelle. I.C., E.G., J.H.M.C. and C.S. deeply thank the SATT Paris-Saclay for support and funding.

References

(1) Pisklak, T. J.; Macías, M.; Coutinho, D. H.; Huang, R. S.; Balkus, K. J. Hybrid Materials for Immobilization of MP-11 Catalyst. *Top Catal* **2006**, *38* (4), 269–278. https://doi.org/10.1007/s11244-006-0025-6.

(2) Lykourinou, V.; Chen, Y.; Wang, X.-S.; Meng, L.; Hoang, T.; Ming, L.-J.; Musselman, R. L.; Ma, S. Immobilization of MP-11 into a Mesoporous Metal–Organic Framework, MP-11@mesoMOF: A New Platform for Enzymatic Catalysis. *J Am Chem Soc* **2011**, *133* (27), 10382–10385. https://doi.org/10.1021/ja2038003.

(3) Stock, N.; Biswas, S. Synthesis of Metal-Organic Frameworks (MOFs): Routes to Various MOF Topologies, Morphologies, and Composites. *Chem Rev* **2012**, *112* (2), 933–969. https://doi.org/10.1021/cr200304e.

(4) Jiang, H.; Alezi, D.; Eddaoudi, M. A Reticular Chemistry Guide for the Design of Periodic Solids. *Nat Rev Mater* **2021**, *6* (6), 466–487. https://doi.org/10.1038/s41578-021-00287-y.

(5) Gkaniatsou, E.; Sicard, C.; Ricoux, R.; Mahy, J. P.; Steunou, N.; Serre, C. Metal-Organic Frameworks: A Novel Host Platform for Enzymatic Catalysis and Detection. *Mater Horiz* **2017**, *4* (1), 55–63. https://doi.org/10.1039/c6mh00312e.

(6) Chen, G.; Huang, S.; Kou, X.; Wei, S.; Huang, S.; Jiang, S.; Shen, J.; Zhu, F.; Ouyang, G. A Convenient and Versatile Amino-Acid-Boosted Biomimetic Strategy for the Nondestructive Encapsulation of Biomacromolecules within Metal–Organic Frameworks. *Angew Chem Inter Ed* **2019**, *58* (5), 1463–1467. https://doi.org/10.1002/anie.201813060.

(7) Wang, X.; Lan, P. C.; Ma, S. Metal–Organic Frameworks for Enzyme Immobilization: Beyond Host Matrix Materials. *ACS Cent Sci* **2020**, *6* (9), 1497–1506. https://doi.org/10.1021/acscentsci.0c00687.

(8) Drout, R. J.; Robison, L.; Farha, O. K. Catalytic Applications of Enzymes Encapsulated in Metal–Organic Frameworks. *Coord Chem Rev* **2019**, *381*, 151–160. https://doi.org/https://doi.org/10.1016/j.ccr.2018.11.009.

(9) Liang, W.; Wied, P.; Carraro, F.; Sumby, C. J.; Nidetzky, B.; Tsung, C.-K.; Falcaro, P.; Doonan, C. J. Metal–Organic Framework-Based Enzyme Biocomposites. *Chem Rev* **2021**, *121* (3), 1077–1129. https://doi.org/10.1021/acs.chemrev.0c01029.

(10) Lyu, F.; Zhang, Y.; Zare, R. N.; Ge, J.; Liu, Z. One-Pot Synthesis of Protein-Embedded Metal–Organic Frameworks with Enhanced Biological Activities. *Nano Lett* **2014**, *14* (10), 5761–5765. https://doi.org/10.1021/nl5026419.

(11) Liang, K.; Ricco, R.; Doherty, C. M.; Styles, M. J.; Bell, S.; Kirby, N.; Mudie, S.; Haylock, D.; Hill, A. J.; Doonan, C. J.; Falcaro, P. Biomimetic Mineralization of Metal-Organic Frameworks as Protective Coatings for Biomacromolecules. *Nat Commun* **2015**, *6* (1), 7240. https://doi.org/10.1038/ncomms8240.

(12) Li, S.; Dharmarwardana, M.; Welch, R. P.; Benjamin, C. E.; Shamir, A. M.; Nielsen, S. O.; Gassensmith, J. J. Investigation of Controlled Growth of Metal–Organic Frameworks on Anisotropic Virus Particles. *ACS Appl Mater Interfaces* **2018**, *10* (21), 18161–18169. https://doi.org/10.1021/acsami.8b01369.

(13) Riccò, R.; Liang, W.; Li, S.; Gassensmith, J. J.; Caruso, F.; Doonan, C.; Falcaro, P. Metal–Organic Frameworks for Cell and Virus Biology: A Perspective. *ACS Nano* **2018**, *12* (1), 13–23. https://doi.org/10.1021/acsnano.7b08056.

(14) Luzuriaga, M. A.; Herbert, F. C.; Brohlin, O. R.; Gadhvi, J.; Howlett, T.; Shahrivarkevishahi, A.; Wijesundara, Y. H.; Venkitapathi, S.; Veera, K.; Ehrman, R.; Benjamin, C. E.; Popal, S.; Burton, M. D.; Ingersoll, M. A.; De Nisco, N. J.; Gassensmith, J. J. Metal–Organic Framework Encapsulated Whole-Cell Vaccines Enhance Humoral Immunity against Bacterial Infection. *ACS Nano* **2021**, *15* (11), 17426–17438. https://doi.org/10.1021/acsnano.1c03092.

(15) Ricco, R.; Pfeiffer, C.; Sumida, K.; Sumby, C. J.; Falcaro, P.; Furukawa, S.; Champness, N. R.; Doonan, C. J. Emerging Applications of Metal–Organic Frameworks. *CrystEngComm* **2016**, *18* (35), 6532–6542. https://doi.org/10.1039/C6CE01030J.

(16) Liao, F. S.; Lo, W. S.; Hsu, Y. S.; Wu, C. C.; Wang, S. C.; Shieh, F. K.; Morabito, J. V.; Chou, L. Y.; Wu, K. C. W.; Tsung, C. K. Shielding against Unfolding by Embedding Enzymes in

Metal-Organic Frameworks via a de Novo Approach. *J Am Chem Soc* **2017**, *139* (19), 6530–6533. https://doi.org/10.1021/jacs.7b01794.

(17) Liang, W.; Xu, H.; Carraro, F.; Maddigan, N. K.; Li, Q.; Bell, S. G.; Huang, D. M.; Tarzia, A.; Solomon, M. B.; Amenitsch, H.; Vaccari, L.; Sumby, C. J.; Falcaro, P.; Doonan, C. J. Enhanced Activity of Enzymes Encapsulated in Hydrophilic Metal–Organic Frameworks. *J Am Chem Soc* **2019**, *141* (6), 2348–2355. https://doi.org/10.1021/jacs.8b10302.

(18) Cases Díaz, J.; Lozano-Torres, B.; Giménez-Marqués, M. Boosting Protein Encapsulation through Lewis-Acid-Mediated Metal–Organic Framework Mineralization: Toward Effective Intracellular Delivery. *Chem Mater* **2022**, *34* (17), 7817–7827. https://doi.org/10.1021/acs.chemmater.2c01338.

(19) Permyakova, A.; Kakar, A.; Bachir, J.; Gkaniatsou, E.; Haye, B.; Menguy, N.; Nouar, F.; Serre, C.; Steunou, N.; Coradin, T.; Fernandes, F. M.; Sicard, C. *In Situ* Synthesis of a Mesoporous MIL-100(Fe) Bacteria Exoskeleton. *ACS Mater Lett* **2023**, *5* (1), 79–84. https://doi.org/10.1021/acsmaterialslett.2c00820.

(20) Gascón, V.; Castro-Miguel, E.; Díaz-García, M.; Blanco, R. M.; Sanchez-Sanchez, M. *In Situ* and Post-synthesis Immobilization of Enzymes on Nanocrystalline MOF Platforms to Yield Active Biocatalysts. *J Chem Technol Biotechnol* **2017**, *92* (10), 2583–2593. https://doi.org/10.1002/jctb.5274.

(21) Hsu, P. H.; Chang, C. C.; Wang, T. H.; Lam, P. K.; Wei, M. Y.; Chen, C. T.; Chen, C. Y.; Chou, L. Y.; Shieh, F. K. Rapid Fabrication of Biocomposites by Encapsulating Enzymes into Zn-MOF-74 via a Mild Water-Based Approach. *ACS Appl Mater Interfaces* **2021**, *13* (44), 52014–52022. https://doi.org/10.1021/acsami.1c09052.

(22) Mirzazadeh Dizaji, N.; Lin, Y.; Bein, T.; Wagner, E.; Wuttke, S.; Lächelt, U.; Engelke, H. Biomimetic Mineralization of Iron-Fumarate Nanoparticles for Protective Encapsulation and Intracellular Delivery of Proteins. *Chem Mater* **2022**, *34* (19), 8684–8693. https://doi.org/10.1021/acs.chemmater.2c01736.

(23) Díaz, J. C.; Giménez-Marqués, M. Alternative Protein Encapsulation with MOFs: Overcoming the Elusive Mineralization of HKUST-1 in Water. *Chem Commun* **2024**, *60* (1), 51–54. https://doi.org/10.1039/D3CC04320G.

(24) Jordahl, D.; Armstrong, Z.; Li, Q.; Gao, R.; Liu, W.; Johnson, K.; Brown, W.; Scheiwiller, A.; Feng, L.; Ugrinov, A.; Mao, H.; Chen, B.; Quadir, M.; Li, H.; Pan, Y.; Yang, Z. Expanding the "Library" of Metal–Organic Frameworks for Enzyme Biomineralization. *ACS Appl Mater Interfaces* **2022**, *14* (46), 51619–51629. https://doi.org/10.1021/acsami.2c12998.

(25) Fan, W.; Wang, K. Y.; Welton, C.; Feng, L.; Wang, X.; Liu, X.; Li, Y.; Kang, Z.; Zhou, H. C.; Wang, R.; Sun, D. Aluminum Metal–Organic Frameworks: From Structures to Applications. *Coord Chem Rev* **2023**, *489*, 215175. https://doi.org/10.1016/J.CCR.2023.215175.

(26) Marrack, P.; McKee, A. S.; Munks, M. W. Towards an Understanding of the Adjuvant Action of Aluminium. *Nat Rev Immunol* **2009**, *9* (4), 287–293. https://doi.org/10.1038/nri2510.

(27) Sicard, C.; Cohen, J. H. M.; Gkaniatsou, E. Immunogenic Composition Containing an Antigen and an Adjuvant Comprising Al-MOFs. C. Sicard, J.H.M. Cohen, WO Pat., PCT/EP2022/058789, 2021.

(28) Christodoulou, I.; Gkaniatsou, E.; Bourdreux, F.; Haouas, M.; Steunou, N.; Patriarche, G.; Djediat, C.; Pagnon-Minot, A.; Lecerf, C.; Lopez, M.; Chereul, E.; Reveil, B.; Audonnet, S.; Kisserli, A.; Tabary, T.; Cohen, J. H. M.; Sicard, C. Al-Fumarate, a Metal-Organic Framework Encapsulating Antigen as a Potent, Versatile and Resorbable Vaccine Adjuvant. *ChemRvix* **2023**, https://doi.org/10.26434/chemrxiv-2023-hhw0t.

(29) a) Férey, G.; Latroche, M.; Serre, C.; Millange, F.; Loiseau, T.; Percheron-Guégan, A. Hydrogen Adsorption in the Nanoporous Metal-Benzenedicarboxylate $M(OH)(O_2C–C_6H_4–CO_2)$ ($M = Al^{3+}$, Cr^{3+}), MIL-53. *Chem. Commun.* **2003**, *24*, 2976–2977. https://doi.org/10.1039/B308903G. b) Loiseau, T.; Serre, C.; Huguenard, C.; Fink, G.; Taulelle, F.; Henry, M.; Bataille, T.; Férey, G. A rationale for the large breathing of the porous aluminum terephthalate (MIL-53) upon hydration. *Chem. Eur. J.*, **2004**, *10* (6), 1373. https://doi.org/10.1002/chem.200305413.

(30) Alvarez, E.; Guillou, N.; Martineau, C.; Bueken, B.; Van de Voorde, B.; Le Guillouzer, C.; Fabry, P.; Nouar, F.; Taulelle, F.; de Vos, D.; Chang, J.; Cho, K. H.; Ramsahye, N.; Devic, T.; Daturi, M.; Maurin, G.; Serre, C. The Structure of the Aluminum Fumarate Metal–

Organic Framework A520. *Angew Chem Inter Ed* **2015**, *54* (12), 3664–3668. https://doi.org/10.1002/anie.201410459.

(31) Matemb Ma Ntep, T. J.; Reinsch, H.; Hügenell, P. P. C.; Ernst, S.-J.; Hastürk, E.; Janiak, C. Designing a New Aluminium Muconate Metal–Organic Framework (MIL-53-Muc) as a Methanol Adsorbent for Sub-Zero Temperature Heat Transformation Applications. *J Mater Chem A* **2019**, *7* (43), 24973–24981. https://doi.org/10.1039/C9TA07465A.

(32) a) Couck, S.; Denayer, J. F. M.; Baron, G. V.; Rémy, T.; Gascon, J.; Kapteijn, F. An Amine-Functionalized MIL-53 Metal-Organic Framework with Large Separation Power for CO2 and CH4. *J Am Chem Soc* **2009**, *131* (18), 6326–6327. https://doi.org/10.1021/JA900555R. b) Min Chin, J.; Chen, E. Y.; Menon, A. G.; Yang Tan, H.; Tzi Sum Hor, A.; Schreyer, M.K.; Xu, J. Tuning the aspect ratio of NH2-MIL-53(Al) microneedles and nanorodsvia coordination modulation. *CrysEngComm*, **2013**, 15, 654-657. https://doi.org/10.1039/C2CE26586A

(33) Loiseau, T.; Serre, C.; Huguenard, C.; Fink, G.; Taulelle, F.; Henry, M.; Bataille, T.; Férey, G. A Rationale for the Large Breathing of the Porous Aluminum Terephthalate (MIL-53) Upon Hydration. *Chem Eur J* **2004**, *10* (6), 1373–1382. https://doi.org/10.1002/chem.200305413.

(34) Loiseau, T.; Lecroq, L.; Volkringer, C.; Marrot, J.; Férey, G.; Haouas, M.; Taulelle, F.; Bourrelly, S.; Llewellyn, P. L.; Latroche, M. MIL-96, a Porous Aluminum Trimesate 3D Structure Constructed from a Hexagonal Network of 18-Membered Rings and M3-Oxo-Centered Trinuclear Units. *J Am Chem Soc* **2006**, *128* (31), 10223–10230. https://doi.org/10.1021/ja0621086.

(35) Benzaqui, M.; Pillai, R. S.; Sabetghadam, A.; Benoit, V.; Normand, P.; Marrot, J.; Menguy, N.; Montero, D.; Shepard, W.; Tissot, A.; Martineau-Corcos, C.; Sicard, C.; Mihaylov, M.; Carn, F.; Beurroies, I.; Llewellyn, P. L.; De Weireld, G.; Hadjiivanov, K.; Gascon, J.; Kapteijn, F.; Maurin, G.; Steunou, N.; Serre, C. Revisiting the Aluminum Trimesate-Based MOF (MIL-96): From Structure Determination to the Processing of Mixed Matrix Membranes for CO2 Capture. *Chem Mater* **2017**, *29* (24), 10326–10338. https://doi.org/10.1021/acs.chemmater.7b03203.

(36) Volkringer, C.; Popov, D.; Loiseau, T.; Férey, G.; Burghammer, M.; Riekel, C.; Haouas, M.; Taulelle, F. Synthesis, Single-Crystal X-Ray Microdiffraction, and NMR Characterizations of the Giant Pore Metal-Organic Framework Aluminum Trimesate MIL-100. *Chem Mater* **2009**, *21* (24), 5695–5697. https://doi.org/10.1021/cm901983a.

(37) Volkringer, C.; Popov, D.; Loiseau, T.; Guillou, N.; Ferey, G.; Haouas, M.; Taulelle, F.; Mellot-Draznieks, C.; Burghammer, M.; Riekel, C. A Microdiffraction Set-up for Nanoporous Metal–Organic-Framework-Type Solids. *Nature Mater 2007 6:10* **2007**, *6* (10), 760–764. https://doi.org/10.1038/nmat1991.

(38) Cadiau, A.; Lee, J. S.; Damasceno Borges, D.; Fabry, P.; Devic, T.; Wharmby, M. T.; Martineau, C.; Foucher, D.; Taulelle, F.; Jun, C.; Hwang, Y. K.; Stock, N.; De Lange, M. F.; Kapteijn, F.; Gascon, J.; Maurin, G.; Chang, J.; Serre, C. Design of Hydrophilic Metal Organic Framework Water Adsorbents for Heat Reallocation. *Advanced Materials* **2015**, *27* (32), 4775–4780. https://doi.org/10.1002/adma.201502418.

(39) Wright, A. K.; Thompson, M. R. Hydrodynamic Structure of Bovine Serum Albumin Determined by Transient Electric Birefringence. *Biophys J* **1975**, *15* (2), 137–141. https://doi.org/10.1016/S0006-3495(75)85797-3.

(40) Haouas, M.; Volkringer, C.; Loiseau, T.; Férey, G., Taulelle, F.; In Situ NMR, Ex Situ XRD and SEM Study of the Hydrothermal Crystallization of Nanoporous Aluminum Trimesates MIL-96, MIL-100, and MIL-110. *Chem Mater* **2012**, *24*(13), 2462–2471, https://doi-org/10.1021/cm300439e

(41) a) Geno, K. A.; Gilbert, G. L.; Song, J. Y.; Skovsted, I. C.; Klugman, K. P.; Jones, C.; Konradsen, H. B.; Nahm, M. H. Pneumococcal Capsules and Their Types: Past, Present, and Future. *Clin Microbiol Rev* **2015**, *28* (3), 871–899. https://doi.org/10.1128/CMR.00024-15. b) Gao, F.; Lockyer, K.; Burkin, K.; Crane T, D.; Boljiano, B.; A physico-chemical assessment of the thermal stability of pneumococcal conjugate vaccine components. *Hum Vaccin Immunother* **2014**, *10*(9), 2744-2753. https://doi.org/10.4161/hv.29696

(42) Duan, P.; Schmidt-Rohr, K. Composite-Pulse and Partially Dipolar Dephased MultiCP for Improved Quantitative Solid-State 13 C NMR. *Journal of Magnetic Resonance* **2017**, *285*, 68–78. https://doi.org/10.1016/j.jmr.2017.10.010.

(43) Haouas, M.; Taulelle, F.; Martineau, C. Recent Advances in Application of 27Al NMR Spectroscopy to Materials Science. *Prog Nucl Magn Reson Spectrosc* **2016**, *94–95*, 11–36. https://doi.org/10.1016/j.pnmrs.2016.01.003.

(44) Massiot, D.; Fayon, F.; Capron, M.; King, I.; Le Calvé, S.; Alonso, B.; Durand, J.; Bujoli, B.; Gan, Z.; Hoatson, G. Modelling One- and Two-dimensional Solid-state NMR Spectra. *Magnetic Resonance in Chemistry* **2002**, *40* (1), 70–76. https://doi.org/10.1002/mrc.984.